Growth of metastable fcc Co on Ni(001)

S. A. Chambers, S. B. Anderson, H. -W. Chen, and J. H. Weaver
Department of Chemical Engineering and Materials Science, University of Minnesota, Minneapolis, Minnesota 55455
(Received 2 September 1986)

We have used high-energy Auger-electron diffraction and associated kinematical scattering calculations to determine that Co, which is hcp at room temperature and atmospheric pressure, can be grown as a stable, unstrained fcc film on Ni(001). Studies of the early stages of growth show that the first monolayer equivalent does not cover the surface uniformly but rather forms two-dimensional patches with limited amounts of a second layer. The second monolayer equivalent adds to the second layer of each patch and provides a limited number of third-layer atoms. When the total Co coverage exceeds two monolayer equivalents, the overlayer coalesces into a continuous fcc film with no detectable strain up to 30 monolayers (the highest coverage studied). For comparison, we have measured angular distributions for Cu/Ni(001) with 0.5 and 1.0 monolayer of Cu. From surface thermodynamic considerations, Cu is expected to wet the surface uniformly. However, Cu also tends to form two-layer-deep patches at a coverage of one monolayer equivalent. These results demonstrate that limited surface mobility is significant in determining the morphology of monolayer metal films, in agreement with theoretical models of overlayer growth behavior.

The correlation between the structure and the properties of ultrathin metal overlayers on single-crystal substrates has received considerable attention recently,[1–12] with particular emphasis on the effects of lattice mismatch and strain on the electronic and magnetic properties of the overlayer. (Analogous effects for semiconductor heterojunctions have also received a great deal of attention.) For example, recent angle-resolved photoemission measurements have distinguished the majority and minority spin bands for metal-metal systems like $p(1\times1)$-Ni/Cu(001) and $p(1\times1)$-Fe/Cu(001), in quantitative agreement with all-electron total-energy calculations.[13–16] Other studies have shown tetragonal distortions in the cubic overlayer to accommodate compressive stresses at the interfaces.[12] Still others have shown the growth of substrate-stabilized overlayers, such as epitaxial bcc Fe and Co on fcc GaAs,[17] and the associated unique properties of the artificial structure. Fundamental to these studies of interfaces is the relationship between the thermodynamic tendencies of the overlayer to assume an equilibrium structure and the kinetic parameters which govern surface mobility of the arriving adatoms. The relationship between substrate temperature, deposition rate, surface diffusion coefficients, and specific surface free energies of formation all influence the composition and structure of the interface.

In order to fully characterize and understand metal overlayers, accurate structural probes are needed. One of the tools recently developed for the structural determination of epitaxial overlayers is high-energy Auger-electron diffraction. As has been demonstrated, this technique is capable of detecting the onset of second- and third-layer formation[6–8] and, with higher angular resolution, lattice contraction and dilation perpendicular to the interface accompanying pseudomorphic growth can be observed.[12]

In this paper we examine the growth of Co on Ni(001) over a wide range of coverages and, for comparison with the low-coverage data, we examine the early stages of Cu growth on Ni(001). We find that both Co and Cu form epitaxial patches when deposited onto the room-temperature substrate at coverages of less than or equal to 1 monolayer (ML) and deposition rates of $\sim$0.5 ML per minute. For Co/Ni(001) we find that Co *LMM* polar angular distributions in the (010) azimuthal plane (perpendicular to the surface) are virtually identical to those of the substrate for coverages between 3 and 30 ML. This demonstrates that the growth mode of Co on Ni is epitaxial, generating an unstrained metastable fcc Co phase at room temperature. Our results are consistent with previous transmission-electron-microscopy (TEM) work which indicated pseudomorphic, dislocation-free epitaxial growth up to 28 ML.[18]

All measurements were performed with an angle-resolved Auger-electron spectrometer employing a single-pass cylindrical mirror energy analyzer (CMA). The energy analyzer had been modified for high angular resolution Auger and low-energy electron diffraction measurements ($\Delta\theta\Delta\phi=2°\times4°$). The two-axis crystal goniometer and the CMA were interfaced to a Digital Equipment Corporation PDP 11/23 microcomputer so that all angular distributions were obtained under high-precision computer control. The system is also equipped with two electron guns, one built into the CMA with an angle of incidence with respect to the polar angle rotation axis of 90° and the other having an angle of incidence of 20° with respect to the polar axis.

The Ni crystal was cut and polished to within 0.5° of the (001) crystallographic plane. It was repetitively Ar-ion sputtered at 500 eV and annealed at $\sim$550 °C to yield a clean, well-ordered surface. Electron beam melted and purified Co was resistively evaporated from a tungsten boat. The system pressure never rose above 2×10^{-10} Torr during evaporation because the source had been extensively outgassed prior to the formation of the interface. The pressure quickly recovered to the base value of $\sim4\times10^{-11}$ Torr. The Co flux was monitored with a quartz crystal oscillator and was adjusted to give a deposi-

tion rate of ~ 0.5 monolayers per minute.

Kinematical scattering calculations[19] were performed on a Cray II, at the University of Minnesota Supercomputer Institute. Free-atom plane-wave scattering factors calculated by Fink and Ingram were interpolated over atomic number and energy to arrive at values used in the present calculation.[20] A 50% reduction in both scattering strengths and inelastic mean free paths taken from empirical values by Seah and Dench[21] was carried out to account for the neglect of spherical-wave and multiple-scattering effects, as discussed elsewhere.[22,23]

In Fig. 1 we show representative *LMM* Auger spectra for the clean Ni(001) substrate (top) and 1-ML-equivalent overlayers of Co (center) and Cu (bottom). The primary beam voltage was 5 kV and the polar angle of emission (θ) was 48° with respect to the surface plane. As can be seen, the *LMM* Auger transitions of Co, Ni, and Cu overlap, thereby limiting which lines can be used in interface studies. For each element, the three dominant lines are assigned to $L_{2,3}M_{2,3}M_{2,3}$, $L_{2,3}M_{2,3}M_{4,5}$, and $L_{2,3}M_{4,5}M_{4,5}$ transitions. These lines move to higher energy in the sequence Co-Ni-Cu in such a way that the second and third lines in the Co series overlap with the first two lines in the Ni series, and the first two lines in the Cu series overlap with the second and third lines in the Ni series. Therefore, only the Co $L_{2,3}M_{2,3}M_{2,3}$ line can be used for low Co coverages of Co/Ni. However, once the Ni $L_{2,3}M_{4,5}M_{4,5}$ line is completely attenuated by the growing overlayer, any of the three Co lines can be used. Likewise, for the low-coverage Cu/Ni interface studies, we are restricted to the Cu $L_{2,3}M_{4,5}M_{4,5}$ line.

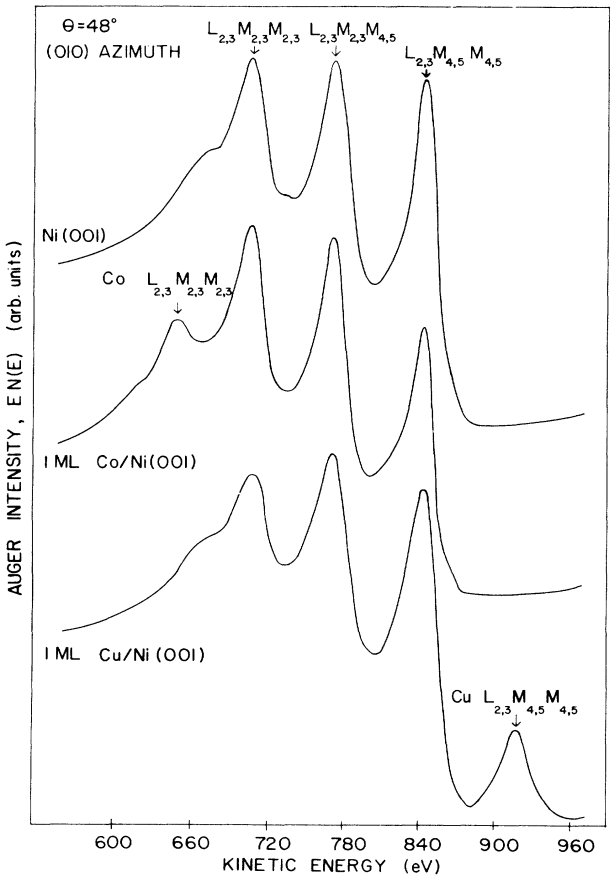

FIG. 1. High-energy *LMM* Auger spectra for Ni(001) (top), 1 ML Co/Ni(001) (middle), and 1 ML Cu/Ni(001) (bottom). The incident electron energy was 5 kV.

In Fig. 2 we show polar angle intensity distributions averaged over the (010) and (100) azimuthal planes for Ni and Co *LMM* emission. At the top, we show the fcc Ni $L_{2,3}M_{4,5}M_{4,5}$ Auger emission profile from the clean surface. Below, we show the evolution of Co *LMM* polar profiles starting with 0.5 ML at the bottom and proceeding to 30 ML near the top. For the low coverages, we used the Co $L_{2,3}M_{2,3}M_{2,3}$ peak. By 10 ML, the Ni $L_{2,3}M_{4,5}M_{4,5}$ line was completely attenuated. Therefore, the peak at 770 eV was due entirely to Co $L_{2,3}M_{4,5}M_{4,5}$ emission, and we used this line for 10 and 30 ML Co overlayers. The clean surface angular distribution shows diffraction-induced intensity maxima characteristic of low-index directions in an fcc metal ([101] at $\theta=45°$ and [001] at $\theta=90°$). These peaks are brought about by simple zeroth-order forward scattering of high-energy Ni Auger electrons from chains of atoms along these directions. The other structures at $\theta=25°$ and $\theta=60°-80°$ are the result of more complex interference phenomena. These features cannot be associated with individual scattering events and their interpretation requires detailed scattering calculations.

The results of Fig. 2 show that a weak Co *LMM* feature appears at $\sim 40°$ by a coverage of 0.5 ML. This feature grows and moves to $\sim 45°$ by 1.0 ML, then grows substantially and narrows by 2.0 ML, at which point a peak develops at 90°. By 3.0 ML, structures at $\sim 23°$ and 60°—80° have developed, and the angular distribution strongly resembles that of the clean surface (compare to Ni polar profile at top of Fig. 2). By 10 ML, the resemblance of the Co angular distribution (now based on $L_{2,3}M_{4,5}M_{4,5}$ emission) is even more striking. Together, these results indicate that Co has grown epitaxially on Ni(001) as a metastable fcc phase. Moreover, the appearance of the peaks along [101] at 1.0 ML and along [001] at 2.0 ML suggest that Co atoms form fcc clusters two and three layers deep by nominal coverages of 1.0 and 2.0 ML, respectively. The interface models to the right of the angular distributions for 0.5, 1.0, and 2.0 ML illustrate what the data suggest. At 0.5 and 1.0 ML the Co atoms form two-dimensional patches with limited amounts of a second layer. By 2.0 ML, the second layer has been built further and limited amounts of a third layer have formed.

To further demonstrate that cluster formation occurs, we show in Fig. 3 azimuthal angular distributions at $\theta=45°$ for the substrate, and 0.5 and 1.0 ML coverages of Co and Cu. Ni $L_{2,3}M_{4,5}M_{4,5}$ emission was used for the substrate profile while Co $L_{2,3}M_{2,3}M_{2,3}$ and Cu $L_{2,3}M_{4,5}M_{4,5}$ emissions were used for Co and Cu overlayers, respectively. In all cases, the angular distributions have been averaged over the four symmetry-equivalent quadrants of the crystal in order to reduce spurious intensity variations, particularly for overlayer emission. This particular choice of angular parameters was chosen to pass through emission directions in which direct forward

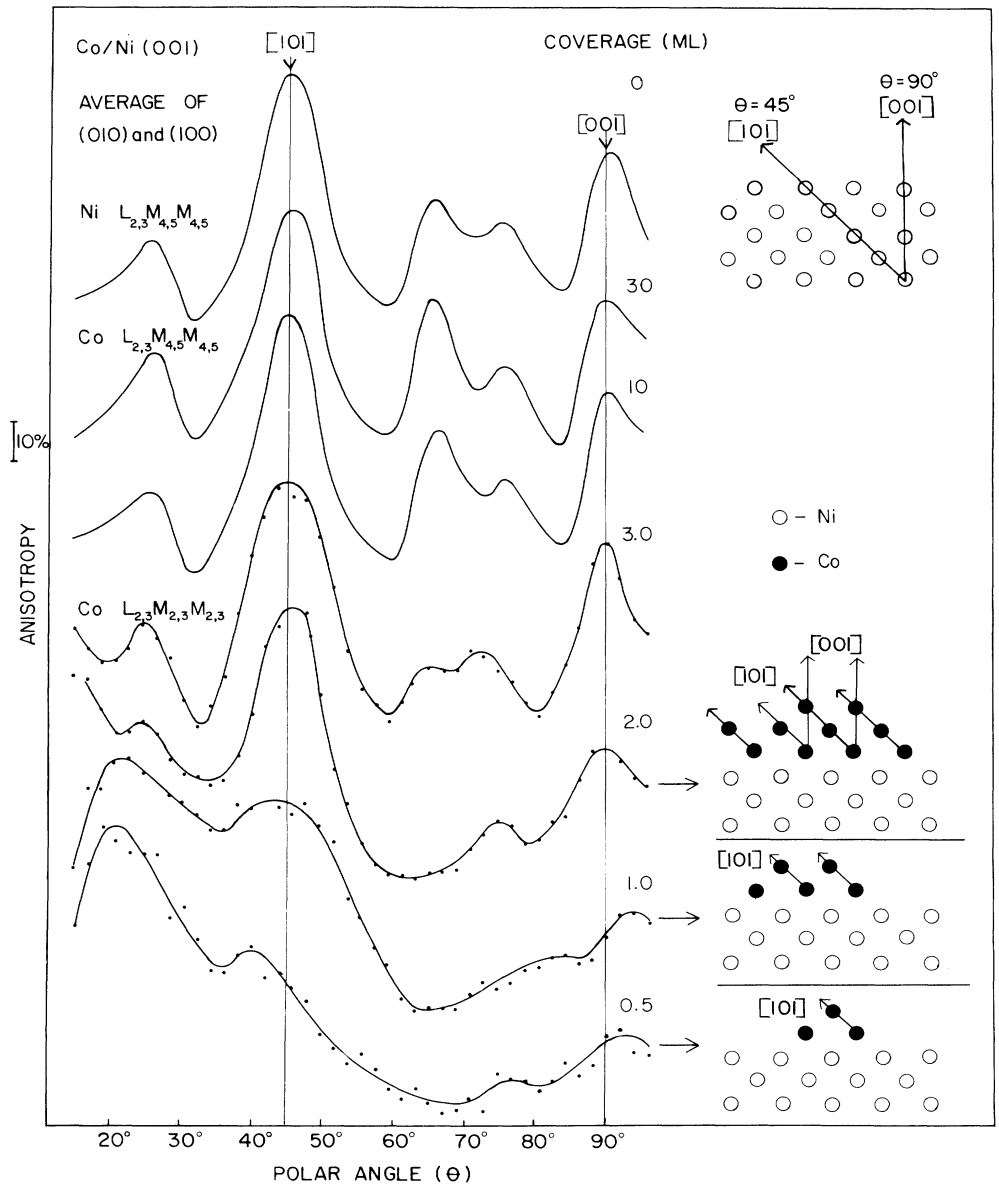

FIG. 2. Polar angle intensity distributions averaged over the (010) and (100) azimuthal planes for Ni(001) and Co/Ni(001) interface over a wide range of coverage. The appearance of diffraction-induced features at $\theta=45°$ for 0.5 and 1.0 ML and at $\theta=90°$ for 2.0 ML betrays the presence of epitaxial clusters at low coverage (see text).

scattering would occur if two-layer-deep clusters were to form on the surface. At $\phi=0°$ and 90°, scattering of electrons emitted from first-layer atoms by second-layer atoms is expected to occur at $\theta=45°$ ([101 at $\phi=0°$ and [011] at $\phi=90°$). Indeed, peaks are seen along these emission directions for both Co and Cu at coverages of 0.5 and 1.0 ML, indicating the formation of a second layer. The anisotropy is lower than that observed for the substrate, as expected. The substrate maxima result because of forward scattering through several layers of atoms along [101] and [011] whereas that for the overlayers is due to scattering through only two layers. In order to place on more solid ground these qualitative remarks about the structure of the evolving Co overlayer, we now turn to comparisons of theoretical and experimental angular distributions for different structural arrangements of Co atoms on a Ni(001) substrate.

We have performed scattering calculations for 1, 2, and 3 layers of Co atoms with 81 atoms in each layer situated epitaxially on a three-layer-deep Ni substrate (also consisting of 81 atoms per layer). In Fig. 4 we compare the calculated polar profiles with experimental data for 1 and 2 ML. As expected, the calculated angular distribution for a 1-ML overlayer does not show any major features along low-index directions, but rather shows only oscillations brought about by the interference pattern of the emitted

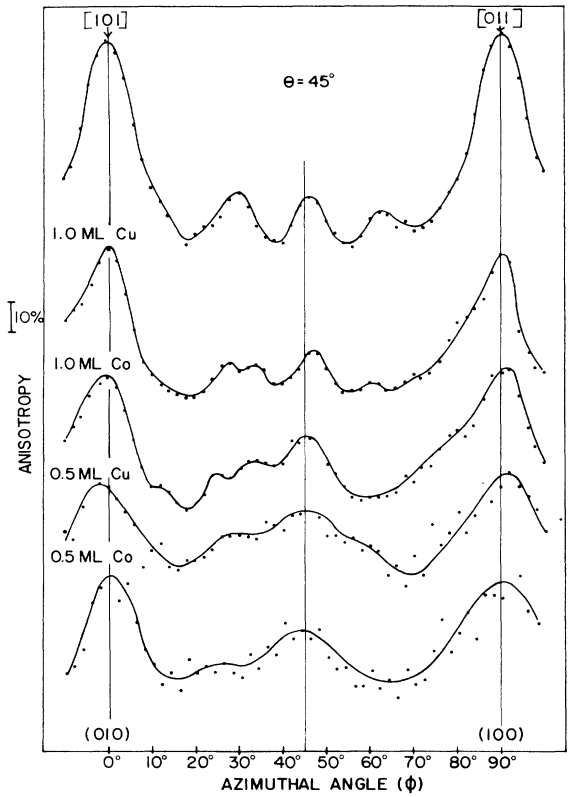

FIG. 3. Azimuthal angle intensity distributions at a 45° polar angle for Ni(001) and 0.5 and 1.0 ML coverages of Co and Cu on Ni(001). The appearance of forward-scattering-induced features at $\phi=0°$ and 90° indicates the presence of two-layer-deep epitaxial patches. The weaker structure between $\phi=20°$ and 70° is the result of more complex interference phenomena involving several atoms.

wave undergoing large-angle scattering events. The vertical scale in these plots is anisotropy, $100(I_{\max}-I)/I_{\max}$, so that the intensity variation with angle is large even though the absolute intensities are very small. The behavior of the theoretical anisotropy with coverage is made especially clear by examining the bottom of the figure in which the calculated intensities are plotted on an absolute scale for the three coverages. As can be seen, the variation of intensity with angle at 1 ML is insignificant compared to that at 2 and 3 ML, since forward scattering produces major features for the latter two coverages.

The calculated profile for 2 ML shows peaks at [101] and [011] corresponding to the presence of second-layer atoms which act as forward scatterers for first-layer atoms. However, there is no calculated peak at [001] because there are no third-layer scatterers directly above first-layer atoms. This feature at [001] does appear in the calculated angular distribution upon the addition of the third layer, confirming the suggestion that some three-layer-deep clusters have formed by a coverage of 2 ML equivalents. Furthermore, there is good reason to believe that at 1 ML equivalent the ratio of second-layer to first-layer atoms is much less than unity. In the calculation, a single atom is picked at the geometric center of each to be the emitter for that particular layer. Since the second layer is complete in the simulation, the emitted electron from the first layer encounters scatterers along [101] and [011], giving rise to the peaks plotted in Fig. 4. If the second layer were not complete, not all first-layer emitters would encounter scatterers along [101] and [011] and the peaks would be correspondingly weaker, as is observed. Similarly, the second ML equivalent of evaporated atoms evidently acts to locally complete the second layer and build a partial third layer. The conclusion that the third layer is not complete on the majority of clusters by a coverage of 2 ML equivalents is reached by using data from Fig. 2 to compare the ratio of the experimental [001] peak height to that of the [101] peak for 2 and 3 ML (0.40 and 0.69, respectively). The increase in this ratio from 2 to 3 ML equivalents suggests that the third monolayer of evaporated atoms acts to further build the third layer of the clusters. It should be noted that the experiment samples a large (~ 1 mm^2) area of the surface compared to typical cluster dimensions. Therefore, we are averaging over large numbers of clusters which undoubtedly possess a range of sizes.

The epitaxial growth of Co on Ni(001) to form an fcc overlayer at room temperature demonstrates that a suitable substrate can be used to grow phases which are not expected to grow under ordinary conditions. Co is hcp at room temperature and atmospheric pressure and undergoes an hcp to fcc phase transition at 417 °C.[24] The enthalpy associated with the phase transition is only 60 cal/mol, suggesting that the thermodynamic stabilities of the two phases are comparable.[25]

The lattice constant of the fcc Co phase is 3.56 Å and there is a compressive lattice misfit of only 1.1% with Ni ($a=3.52$ Å). It is noteworthy that upon formation of the epitaxial overlayer, we detected no tetragonal expansion of the Co lattice in the direction normal to the interface as we did for the Cu/Ni(001) system (2.6% compressive misfit).[12] Such an expansion is expected in response to the contraction necessary in the plane of the interface for pseudomorphic growth to occur and the tendency of the overlayer material to maintain its bulk density. In the case of Cu/Ni(001), this change was detected by a shift in the polar angle at which the peak along [101] occurred in the (010) azimuth. The shift amounted to $1.3\pm0.2°$ for Cu coverages up to 7 ML. Since the results of Fig. 2 show no analogous shift, we conclude that the fcc Co overlayer grows with nearly perfect epitaxy for at least 30 ML. The density of epitaxial fcc Co on Ni(001) is 8.97 g/cm^3, compared to bulk values of 8.90 and 8.67 g/cm^3 for the room temperature hcp and high-temperature fcc phases, respectively.[26]

The tendency of Co and Cu to form ordered, epitaxial patches of nonuniform thickness at low coverages on Ni(001) is probably the result of limited surface mobility when the substrate is at room temperature, as in the present work. In thermodynamic terms, the mode of growth depends on the specific surface free energies of the substrate, the overlayer, and the interfacial layer. In simplest terms, the condition for equilibrium growth of an epitaxial film is that $\Delta\gamma\equiv\gamma_o+\gamma_i-\gamma_s\leq 0$ where $\gamma_s,\gamma_o,\gamma_i$ are the specific surface free energies of the substrate, the

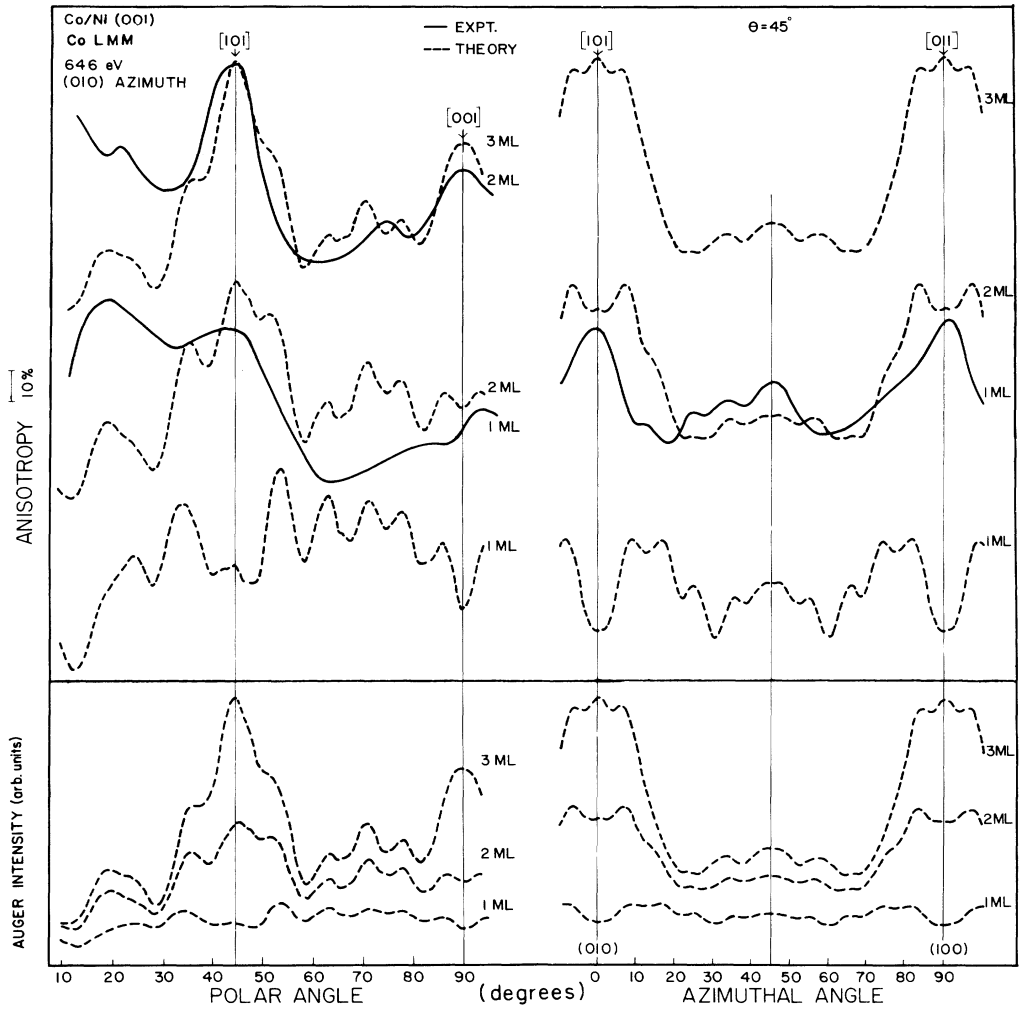

FIG. 4. Comparison of experimental and theoretical angular distributions for the Co/Ni(001) interface at low coverages using the Co $L_{2,3}M_{2,3}M_{2,3}$ Auger intensity. The vertical scale for the top panels is normalized intensity or anisotropy, defined as $100(I_{\max}-I)/I_{\max}$. The curves in the bottom panels are plotted in absolute intensity units.

overlayer, and the interfacial layer.[27,28] For ultralow coverages, the interfacial layer is in effect the overlayer, so that the condition for uniform wetting by the first layer is given by $\Delta\gamma=\gamma_o-\gamma_s\leq 0$. Using specific surface free energies computed by Mazey and Giber,[29] $\Delta\gamma$ becomes 0.345 and -0.430 J/m^2 for the Co/Ni and Cu/Ni interfaces, respectively. For the Ni(001) surface atom number density, these numbers are equivalent to 0.134 and -0.167 eV/atom for Co/Ni and Cu/Ni, respectively. Therefore, uniform wetting by the first monolayer is expected for Cu but not for Co. The fact that neither element uniformly wets Ni(001) can then be explained by limited surface mobility of the arriving adatoms rather than thermodynamic considerations. Upon arrival at the surface, each atom is likely to condense on the first energetically favorable site it encounters, whether that site is on the substrate or on an island of adsorbate. At low coverages the result is patches; however, as coverage proceeds it is expected that the substrate will be completely covered and that epitaxy will continue until the misfit strain is relieved by the introduction of dislocations which, according to TEM measurements,[18] occurs at 50 Å (28 ML).

The description of overlayer development we present is consistent with theoretical calculations by Kashchiev, who developed a model for layer growth on dislocation-free surfaces by treating the growth kinetics of the interfacial layer as independent of, and different from, the kinetics of subsequent layer growth.[30] For heteroepitaxy, the mode of growth was shown to depend on the ratio τ_1/τ_2, where τ_1 and τ_2 are the characteristic times required to complete the first and second layers, respectively. Moreover, the ratio τ_1/τ_2 was shown to depend on the condensing beam supersaturation $\Delta\mu$, defined as $kT\ln(P/P_0)$, where T is the substrate temperature, P_0 is the vapor pressure of the condensing material at the temperature of the substrate, and P is the effective pressure of the condensing beam. This theoretical work and associated Monte Carlo simulations showed that for both homoepitaxy (for which $\Delta\gamma\equiv 0$) and heteroepitaxy (with $\Delta\gamma>0$), statistical fluctuations in film thickness will occur in the

case of zero surface mobility.[31] The mean overlayer thickness required to cover 99% of the substrate was calculated to vary from 1 to 25 monolayer equivalents, depending on the values of $\Delta\mu$ and $\Delta\gamma$. Although there is surface mobility in the experiment at a substrate temperature of 20 °C, it is probably quite low for Co and Cu on Ni(001), leading to a distribution of local overlayer thicknesses across the surface.

In conclusion, we have examined the mode of growth of Co on Ni(001) and have found that the Ni substrate induces the formation of a metastable fcc phase for coverages at least as high as 30 ML. At low coverages the arriving Co adatoms form fcc epitaxial, ordered patches which coalesce into a continuous fcc film by ~ 3 ML. The clusters are one to two layers in thickness after 1 ML equivalent has been deposited and a third layer begins to form after the addition of 2 ML equivalents. Similarly, Cu coverages up to 1 ML form epitaxial clusters up to two layers thick on Ni(001) and do not wet the surface uniformly, as expected from free-energy calculations for the process. Deviations of the growth mode from what is expected on thermodynamic grounds is explained by limited surface mobility. This work demonstrates that high-energy Auger-electron diffraction is a powerful probe of overlayer thickness distribution at ultralow coverages. For most other experimental probes, the mode of growth described above would be indistinguishable from classical Frank—van der Merwe growth in the low-coverage regime.

We are pleased to acknowledge helpful discussions with Professor W. W. Gerberich. This work was supported by the National Science Foundation under Grants No. DMR-82-16489 and No. 86-10837. Computational time on the Cray was generously provided by the Minnesota Supercomputer Institute.

[1]I. K. Schuller, Phys. Rev. Lett. **44**, 1597 (1980).
[2]W. P. Lowe, T. W. Barbee, Jr., T. H. Geballe, and D. B. McWhan, Phys. Rev. B **24**, 6193 (1981).
[3]W. C. Marra, P. H. Fuoss, and P. E. Eisenberger, Phys. Rev. Lett. **49**, 1169 (1982).
[4]F. Comin, P. H. Citrin, P. Eisenberger, and J. E. Rowe, Phys. Rev. B **26**, 7060 (1982).
[5]Y. Kuk, L. C. Feldman, and P. J. Silverman, Phys. Rev. Lett. **50**, 511 (1983).
[6]W. F. Egelhoff, Jr., Phys. Rev. B **30**, 1052 (1984).
[7]W. F. Egelhoff, Jr., J. Vac. Sci. Technol. A **2**, 350 (1984).
[8]E. L. Bullock and C. S. Fadley, Phys. Rev. B **31**, 1212 (1984).
[9]S. A. Chambers, S. B. Anderson, and J. H. Weaver, Phys. Rev. B **32**, 4872 (1984).
[10]P. Roubin, D. Chandesris, E. Rossi, L. Lecante, M. C. Desjonquéres, and G. Tréglia, Phys. Rev. Lett. **56**, 1272 (1986).
[11]S. Brennan, P. H. Fuoss, and P. Eisenberger, Phys. Rev. B **33**, 3678 (1986).
[12]S. A. Chambers, H.-W. Chen, I. M. Vitomirov, S. P. Anderson, and J. H. Weaver, Phys. Rev. B **33**, 8810 (1986).
[13]M. A. Thompson and J. L. Erskine, Phys. Rev. B **31**, 6832 (1985); M. F. Onellion, C. L. Fu, M. A. Thompson, J. L. Erskine, and A. J. Freeman, *ibid.* **33**, 7322 (1986).
[14]D. Wang, A. J. Freeman, and H. Krakauer, Phys. Rev. B **24**, 1126 (1981).
[15]J. Tersoff and L. M. Falicov, Phys. Rev. B **26**, 6186 (1982); **25**, 2959 (1982).
[16]H. Huang, Z. Zhu, and J. Hermanson, Phys. Rev. B **29**, 2270 (1984).
[17]S. A. Chambers, F. Xu, H.-W. Chen, I. M. Vitomirov, S. B. Anderson, and J. H. Weaver, Phys. Rev. B **34**, 6605 (1986); F. Xu, J. J. Joyce, M. W. Ruckman, H.-W. Chen, F. Boscherini, D. M. Hill, S. A. Chambers, and J. H. Weaver Phys. Rev. B **35**, 2375 (1987); G. A. Prinz, Phys. Rev. Lett. **54**, 1051 (1985).
[18]W. A. Jesser and J. W. Matthews, Acta. Metall. **16**, 1307 (1968).
[19]C. S. Fadley in *Progress in Surface Science*, edited by S. G. Davison (Pergamon, New York, 1984), Vol. 16, pp. 327—365.
[20]M. Fink and J. Ingram, At. Data **4**, 129 (1972).
[21]M. P. Seah and W. A. Dench, Surf. Int. Anal. **1**, 2 (1979).
[22]S. Y. Tong, H. C. Poon, and D. R. Snider, Phys. Rev. B **32**, 2096 (1985).
[23]S. M. Goldberg, R. J. Baird, S. Kono, N. F. T. Hall, and C. S. Fadley, J. Electron Spectrosc. Relat. Phenom. **21**, 1 (1980); R. Trehan and C. S. Fadley, *ibid.* (to be published).
[24]J. B. Hess and C. S. Barrett, J. Met. **4**, 645 (1952).
[25]Cobalt Information Center, "Data on Cobalt," Columbus, OH, 1958.
[26]F. R. Morral, J. Met. **10**, 662 (1958).
[27]E. Bauer, Appl. Surf. Sci. **11/12**, 479 (1982).
[28]E. Bauer and J. H. van der Merwe, Phys. Rev. B **33**, 3657 (1986).
[29]L. Z. Mezey and J. Giber, Jpn. J. Appl. Phys. **21**, 1569 (1982).
[30]D. Kashchiev, J. Cryst. Growth **40**, 29 (1977).
[31]D. Kashchiev, J. P. van der Eerden, and C. van Leeurven, J. Cryst. Growth **40**, 47 (1977).